Jour. Korean Earth Science Society, v. 25, no. 1, p. 22–31, January 2004

# Effect of Intermediate Principal Stress on Rock Fractures

**Chandong Chang***

Department of Geology and Earth Environmental Sciences, Chungnam National University, Daejeon, 305-764, Korea

**Abstract:** Laboratory experiments were conducted in order to find effects of the intermediate principal stress $\sigma_2$ on rock fractures and faults. Polyaxial tests were carried out under the most generalized compressive stress conditions, in which different magnitudes of the least and intermediate principal stresses $\sigma_3$ and $\sigma_2$ were maintained constant, and the maximum stress $\sigma_1$ was increased to failure. Two crystalline rocks (Westerly granite and KTB amphibolite) exhibited similar mechanical behavior, much of which is neglected in conventional triaxial compression tests in which $\sigma_2 = \sigma_3$. Compressive rock failure took the form of a main shear fracture, or fault, steeply dipping in $\sigma_3$ direction with its strike aligned with $\sigma_2$ direction. Rock strength rose significantly with the magnitude of $\sigma_2$, suggesting that the commonly used Mohr-type failure criteria, which ignore the $\sigma_2$ effect, predict only the lower limit of rock strength for a given $\sigma_3$ level. The true triaxial failure criterion for each of the crystalline rocks can be expressed as the octahedral shear stress at failure as a function of the mean normal stress acting on the fault plane. It is found that the onset of dilatancy increases considerably for higher $\sigma_2$. Thus, $\sigma_2$ extends the elastic range for a given $\sigma_3$ and, hence, retards the onset of the failure process. SEM inspection of the micromechanics leading to specimen failure showed a multitude of stress-induced microcracks localized on both sides of the through-going fault. Microcracks gradually align themselves with the $\sigma_1 - \sigma_2$ plane as the magnitude of $\sigma_2$ is raised.

Keywords: intermediate principal stress, polyaxial test, crystalline rock, fracture, strength

## Introduction

Understanding of rock fracture mechanism and mechanical properties such as strength and deformability is fundamental for solving many geomechanical/geophysical problems (e.g. analysis of earthquake and faulting mechanism, estimation of in situ stress magnitude, rational design of rock engineering structures). Fractures and faults in rocks have been studied for centuries because of the need to design safe excavations for extracting minerals from the earth, and for the purpose of using hard rock as a building material (Scholz, 1990). But it was only in the last century that rigorous formulations of rock strength were made, based on the physics of the phenomenon and supported by experimental results. Rock strength is the maximum stress that it can support under specified conditions and is commonly represented by strength criteria. The most widely used criteria are based on the hypothesis that the intermediate principal stress $\sigma_2$ has no role in the process of brittle fracture leading to failure (for example, the Mohr-Coulomb (Jaeger and Cook, 1979); Hoek and Brown, 1980; Ashby and Sammis, 1990). Thus, the commonly used method of determining the deformability and strength of rocks is the conventional 'triaxial' testing of cylindrical samples subjected to uniform lateral load or confining pressure (i.e. $\sigma_2 = \sigma_3$).

However, numerous field measurements have confirmed that the state of stress in the Earth's crust is typically anisotropic (e.g. McGarr and Gay, 1978), in which all three principal stresses are unequal or 'true triaxial' ($\sigma_1 \neq \sigma_2 \neq \sigma_3$). Moreover, when an original state of stress is disturbed by human activity such as excavation of a cavern or a tunnel, or drilling of a wellbore, principal stresses tend to become even more differential. In particular, it was discovered on several occasions that Mohr-type failure criteria gave unreasonable results in some spe-

*E-mail: cchang@cnu.ac.kr
Tel: 82-42-821-6430
Fax: 82-42-822-7661

cific situations (for example, Vernik and Zoback, 1992; Ewy, 1998). In these cases, it was revealed that a correct analysis was feasible only using a criterion that invoked all three principal stresses.

Laboratory studies on rock fractures and faults under true triaxial stress conditions ($\sigma_1 \geq \sigma_2 \geq \sigma_3$) have been carried out by a limited number of researchers (Mogi, 1971; Reches and Dieterich, 1983; Takahashi and Koide 1989). The general finding in these works was that the intermediate principal stress has a significant effect on rock strength and failure behavior. However, because of practical difficulties in designing experimental apparatus that enables the application of the three independent principal stresses, the experimental study on this issue is scarce. In addition, all of the previous experiments conducted until recently were limited to relatively weak sedimentary-based rocks.

In the present study, a further investigation on the effect of $\sigma_2$ on rock fractures was made in two very hard crystalline rocks (granite and amphibolite). Laboratory true triaxial tests were carried out using a sophisticate polyaxial loading apparatus (Chang and Haimson, 2000). This paper describes briefly the equipment, and reports on the experimental results, including deformability, strength, and micromechanics of fracture under the generalized stress condition, with a special attention to the effect of the intermediate principal stress.

## Rocks Tested

Two crystalline rocks were tested: Westerly granite and KTB amphibolite. Westerly granite is a fine to medium grained Late Pennsylvanian to Permian crystalline rock found mainly in the southeast area of Rhode Island, USA (Quinn, 1954). Its mineral composition is: 28% quartz, 36% microcline, 31% plagioclase, and 5% biotite (Wawersik and Brace, 1971). Its physical properties are characterized by high strength, very low porosity, almost complete isotropy, elastic linearity, and homogeneity (Krech et al., 1974). The mechanical properties of Westerly granite have been tested by a large number of experimentalists (Brace, 1964; Brace et al., 1966; Wawersik and Brace, 1971; Wong, 1982; Lockner et al., 1991). However, no known attempt had been made to investigate rock strength and deformability of Westerly granite under true triaxial stress conditions.

The KTB amphibolite was extracted from the super deep scientific borehole drilled by the German Continental Deep Drilling Program (KTB) in Bavaria, Germany. Amphibolite is the dominant rock in the hole between 3 and 7 km depth, and the samples used in this study come from a depth of 6.4 km. The KTB amphibolite is a fine-grained massive metamorphic rock. The mineral composition is: 58% amphibole, 25% plagioclase, 5% garnet, 2% biotite, and 7% minor opaque minerals (Chang and Haimson, 2000). It is characterized by high strength, some inhomogeneity, and very low porosity (Rauen and Winter, 1995). Basic mechanical properties determined by uniaxial and triaxial tests demonstrate near isotropy and linear elasticity (Vernik et al., 1992; Röckel and Natau, 1995).

## Experimental Methods and Procedures

The apparatus used for the application of three mutually perpendicular high compressive loads onto rectangular prismatic specimens consists of two main parts: a pressure vessel and a biaxial cell (Fig. 1). The rock specimen ($2 \times 2 \times 4$ cm) is inserted inside of the pressure vessel and is subjected to a longitudinal load, $\sigma_1$, and one lateral load, $\sigma_2$ (capacity of both 1.6 GPa), applied through high-strength metal anvils, as well as to a second lateral load applied directly by the confining fluid pressure, $\sigma_3$ (capacity 0.4 GPa). Rock specimen is coated with a thin layer of polyurethane to prevent permeation of the confining fluid. The pressure vessel fits inside the biaxial cell, which applies hydraulically activated loads to the two pairs of anvils. All three loads are servo controlled. During each test, strains in the

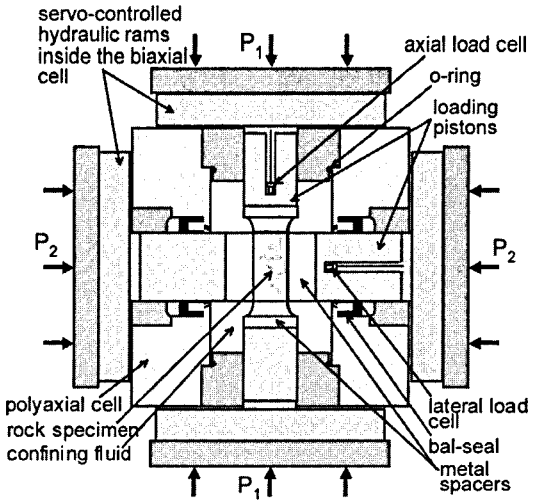


**Fig. 1.** Schematics of the polyaxial cell showing load transmission from the biaxial apparatus ($P_1$ and $P_2$) to rock specimen. The load in the third direction is applied directly by the confining fluid pressure.

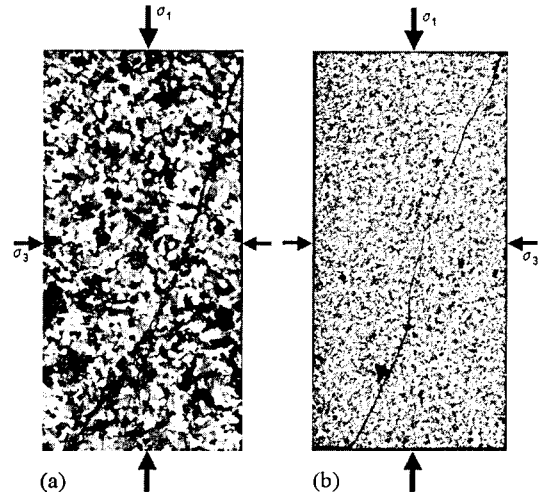


**Fig. 2.** Profiles of fractured specimens along a plane normal to $\sigma_2$, showing steeply inclined faults dipping in the $\sigma_3$ direction: (a) Westerly granite, (b) KTB amphibolite.

specimen are also measured in the three principal stress directions through strain gages (strain measurements in $\sigma_1$ and $\sigma_2$ directions) and strain-gaged beam (strain measurement in $\sigma_3$ direction).

Several sets of true triaxial tests were conducted in each of the two rocks. Tests were run on dry specimens at ambient temperature. Each set comprised of six to ten tests in which the least principal stress was kept constant throughout and the intermediate principal stress $\sigma_2$ was varied from test to test. The range of $\sigma_3$ was from 0 to 100 MPa in Westerly granite and to 150 MPa in KTB amphibolite, and that of $\sigma_2$ was from $\sigma_2=\sigma_3$ to $\sigma_2>5\sigma_3$. Each specimen was inserted in the polyaxial cell and subjected first to linearly increasing hydrostatic loading. As $\sigma_3$ and then $\sigma_2$ reached their preset magnitudes, they were kept constant for the remainder of the test. Thereafter, the maximum stress $\sigma_1$ was raised to failure and beyond by controlling the least principal strain at a constant rate of $5\times10^{-6}$ $s^{-1}$.

## Rock Strength

A common visual observation in test results is that crystalline rocks, as represented by Westerly granite and KTB amphibolite, is that brittle fracture takes the final form of a shear band that appears as a steeply inclined fault plane, striking parallel to $\sigma_2$ direction and dipping in the $\sigma_3$ direction, regardless of the magnitudes of the applied stresses. This failure type is generally similar to that observed in conventional triaxial tests, except that true triaxial loading confirms the expectation that the strike direction of the fault plane is along $\sigma_2$ (Fig. 2).

Test results showing the state of stress at failure in the two crystalline rocks are shown in Fig. 3, in which the true triaxial strengths $\sigma_1$ as a function of the applied $\sigma_2$ were plotted for different constant values of $\sigma_3$. Experiments in which the least and intermediate principal stresses were equal (conventional triaxial tests) reveal a typical monotonic increase in the strength as $\sigma_2=\sigma_3$ was raised from 0 to 150 MPa (see solid lines in Fig. 3). Plotted separately as $\sigma_1$ vs. $\sigma_2=\sigma_3$, the curve best-fitting the experimental points represents the Mohr strength criterion for each rock.

Fig. 3 demonstrates the similarity between the two crystalline rocks with respect to the dependence of $\sigma_1$ at failure as a function of the intermediate principal stress $\sigma_2$. As the magnitude of the latter increased beyond that of $\sigma_3$, the compressive

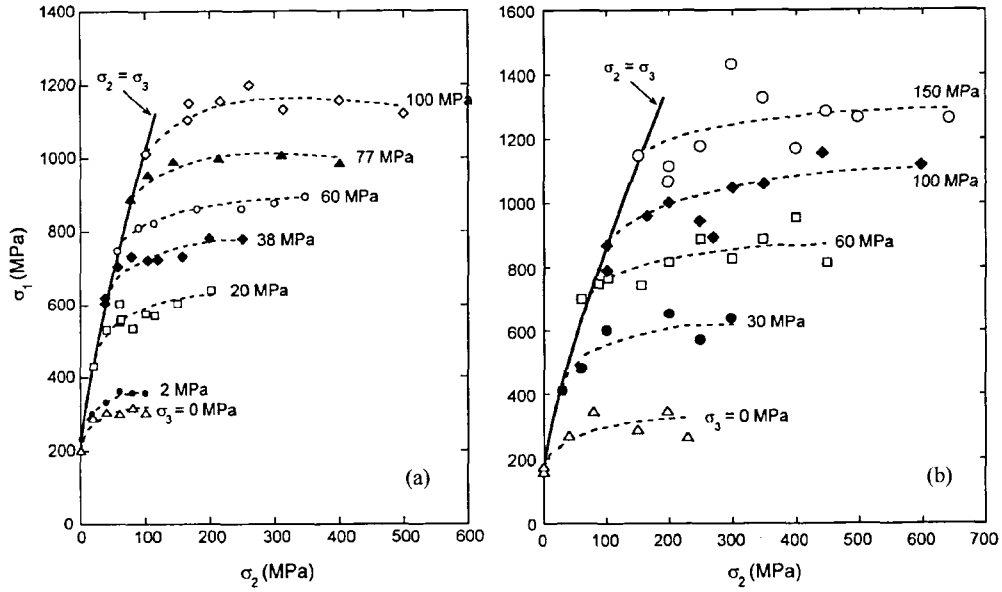


**Fig. 3.** Relationship between peak $\sigma_1$ and $\sigma_2$ for different constant magnitudes of $\sigma_3$ in (a) Westerly granite, and (b) KTB amphibolite. The solid line is the best fit curve to experimental points when $\sigma_2 = \sigma_3$, i.e. the Mohr criterion. Dashed lines show the trend of the true triaxial strength as $\sigma_2$ increases.

strength in both rocks was always higher than that when $\sigma_2 = \sigma_3$. Despite the similarity of behavior between the two crystalline rocks tested, it is evident from Fig. 3 that the KTB amphibolite experimental points are considerably more scattered than those in the Westerly granite. This is probably the result of the greater inhomogeneity and limited anisotropy of the amphibolite (Vernik et al., 1992). Nonetheless, the increase in strength as a function of $\sigma_2$ for constant $\sigma_3$ is quite obvious.

The dashed lines in Fig. 3 represent trends in the variation of the true triaxial strength $\sigma_1$ with the magnitude of $\sigma_2$ for each set of tests in which $\sigma_3$ was held constant. They reveal a rise in $\sigma_1$ with the magnitude of $\sigma_2$ until a plateau is reached where strength appears to level off. This behavior supports Wiebols and Cook (1968) theory, based on the strain energy stored in a rock body due to sliding along microcracks, which predicts that when $\sigma_3$ is held constant and $\sigma_2$ is increased from $\sigma_2 = \sigma_3$ to $\sigma_2 = \sigma_1$, the compressive strength first increases, reaches a maximum at some value of $\sigma_2$ and then decreases but always to a level higher than that obtained in a conventional triaxial test. However, for the ranges of $\sigma_2$ used, there is no clear trend towards a decrease in strength in either of the rocks. The results reported here are also in support of previous observations in Dunham dolomite by Mogi (1971).

As shown in Fig. 3, the true triaxial compressive strength $\sigma_1$ increases by as much as 50% or more over the commonly used conventional triaxial strength (Mohr-based strength criterion), depending on the $\sigma_2$ magnitude. The increase in strength is less pronounced at higher magnitudes of $\sigma_3$, but even for the highest least principal stress the true triaxial strength is larger than that inferred from the Mohr criterion by nearly 20%. Test results shown in Fig. 3 strongly suggest that in crystalline rocks Mohr-based criteria (such as Mohr, Mohr-Coulomb, Hoek and Brown) are only correct for the special case of in situ stress conditions in which $\sigma_2 = \sigma_3$, but are not representative of strength under more general, and more realistic, in situ stress conditions in which all three principal in situ stresses differ in magnitude. In other words, the Mohr-based strength

criteria represent only the lower limit of compressive strength in crystalline rocks for a given least principal stress. Since in situ measurements rarely indicate that two of the in situ principal stresses are equal (McGarr and Gay, 1978), Mohr-based criteria appear to yield overly conservative strength estimates.

Attempts were made to establish a unifying strength criterion for each tested rock that would represent the experimental points shown in Fig. 3. Several rock failure criteria were considered which incorporate all three principal stresses (Nadai 1950, Freudenthal 1951, Drucker and Prager 1952). These criteria are of the form:

$$\tau_{oct} = f(\sigma_{oct}) \quad (1)$$

where $\tau_{oct}$ is the octahedral shear stress, equal to $[(\sigma_1-\sigma_2)^2+(\sigma_2-\sigma_3)^2+(\sigma_3-\sigma_1)^2]^{0.5}/3$, $\sigma_{oct}$ is the octahedral normal stress, equal to $(\sigma_1+\sigma_2+\sigma_3)/3$, and $f$ is a monotonically increasing function. None of these criteria seemed to correctly fit the strength data in Fig. 3.

Mogi (1971) noted that the above criteria, for which the independent variable is the three-dimensional mean normal stress $\sigma_{oct}$, were more appropriate for characterizing yielding that occurs over the entire volume of rock. The brittle failure of the crystalline rock was, however, in the form of localized shearing along a single plane striking in the $\sigma_2$ direction. For that failure mechanism, Mogi proposed that a more appropriate independent variable in the above criterion is obtained by downgrading $\sigma_{oct}$ to its two-dimensional form, $(\sigma_1+\sigma_3)/2$, which represents the mean stress acting on the failure plane:

$$\tau_{oct} = f[(\sigma_1+\sigma_3)/2]. \quad (2)$$

The strength data in both rocks are strikingly well represented by Mogi's (1971) brittle failure criterion in the form of monotonically increasing functions, as demonstrated by Fig. 4. The true triaxial strength criterion given by equation 2 is clearly more general than the Mohr-based criteria, and includes conventional triaxial test results as just a special case.

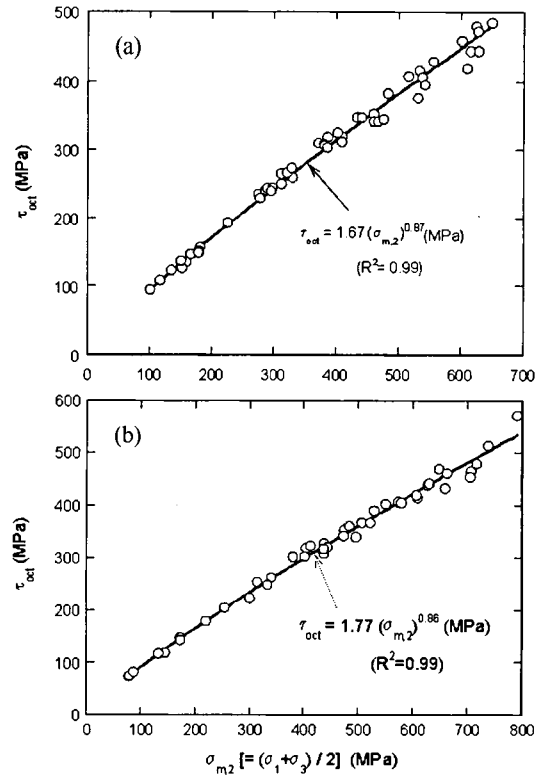


**Fig. 4.** True triaxial strength criterion best-fitting our experimental results, in the form of the octahedral shear stress $\tau_{oct}$ as a function of the mean normal stress acting on the fault plane $\sigma_{m,2}$: (a) Westerly granite, (b) KTB amphiblolite.

## Fracture Angle

For each tested rock samples, the strike and dip of the induced fault plane were carefully measured. Despite its roughness and local inclination variations, an approximate fault plane attitude could be determined within an error of few degrees. The strike was consistently (within ±20°) aligned with the direction of $\sigma_2$. The dip was always steeper than 45° and oriented towards $\sigma_3$. Another major effect of the intermediate principal stress was that the fracture angle for the same $\sigma_3$ increased as the level of $\sigma_2$ was raised (Fig. 5). The trend is similar in both rocks.

Within the $\sigma_2$ ranges tested fracture dip angles

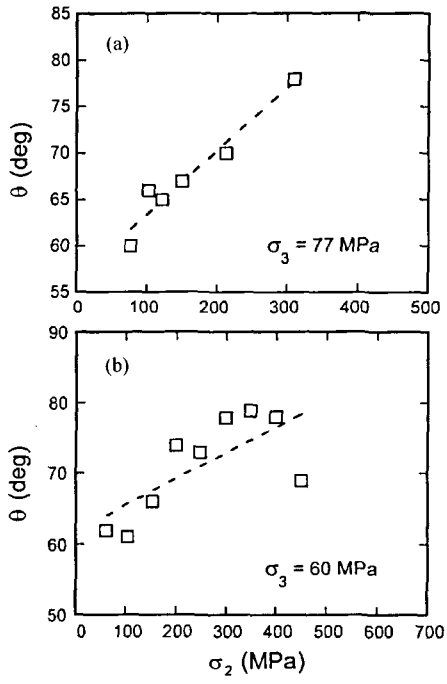


**Fig. 5.** Typical variation of fault dip θ with the magnitude of the intermediate principal stress $\sigma_2$ for a constant least principal stress $\sigma_3$ in (a) Westerly granite and (b) KTB amphibolite.

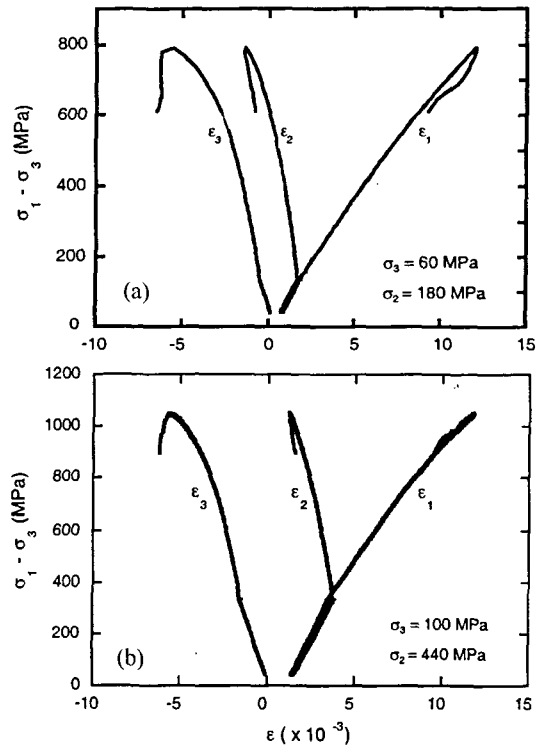


**Fig. 6.** Stress-strain curves under true triaxial loading in (a) Westerly granite and (b) KTB amphibolite. $\sigma_1$, $\sigma_2$, and $\sigma_3$ are strains measured in the $\sigma_1$, $\sigma_2$, and $\sigma_3$ diections, respectively.

increased by substantial amounts (up to 20°) from their base values when $\sigma_2 = \sigma_3$. Similar results were obtained by Mogi (1971) in Dunham dolomite. The mechanism responsible for this mechanical behavior is not clearly understood. However, the implication of this behavior regarding to true triaxial rock strength can be described as follows. For a given applied stress condition, the magnitude of shear stress varies depending on the orientation of the plane on which it acts. The shear stress is maximized on the plane that bisects the angle between $\sigma_1$ and $\sigma_3$, i.e. 45° from the largest principal stress direction. The shear stress decreases as the plane becomes steeper. As rock fracture occurs along a plane inclined at a steeper angle, it requires a higher magnitude of $\sigma_1$ to have the shear stress on the plane reach the critical level leading to failure. Therefore, the increasing intermediate principal stress magnitude tends to raise the peak $\sigma_1$ by steepening the fracture plane, which is manifested by increase in rock strength.

## Stress-Strain Relationship

Fig. 6 shows typical stress-strain records in both rocks. The lower segment of the curves represents the stage in which both $\sigma_1$ and $\sigma_2$ were raised while $\sigma_3$ was kept constant. The remainder of each record gives the stress-strain relationships between $(\sigma_1 - \sigma_3)$ and each of the measured strains for constant $\sigma_2$ and $\sigma_3$, as the strain rate in the $\sigma_3$ direction is raised at a constant rate. It is noted that in both the Westerly granite and the KTB amphibolite all three stress-strain curves are quasi-linear for the first half to two thirds of the stress range in this segment. At higher stress levels, these stress-strain relationships show increasing softening of the rocks. However, the stress-strain behavior in the $\sigma_3$ direction is significantly more nonlinear, suggesting that most of the stress-induced microcracks, leading to

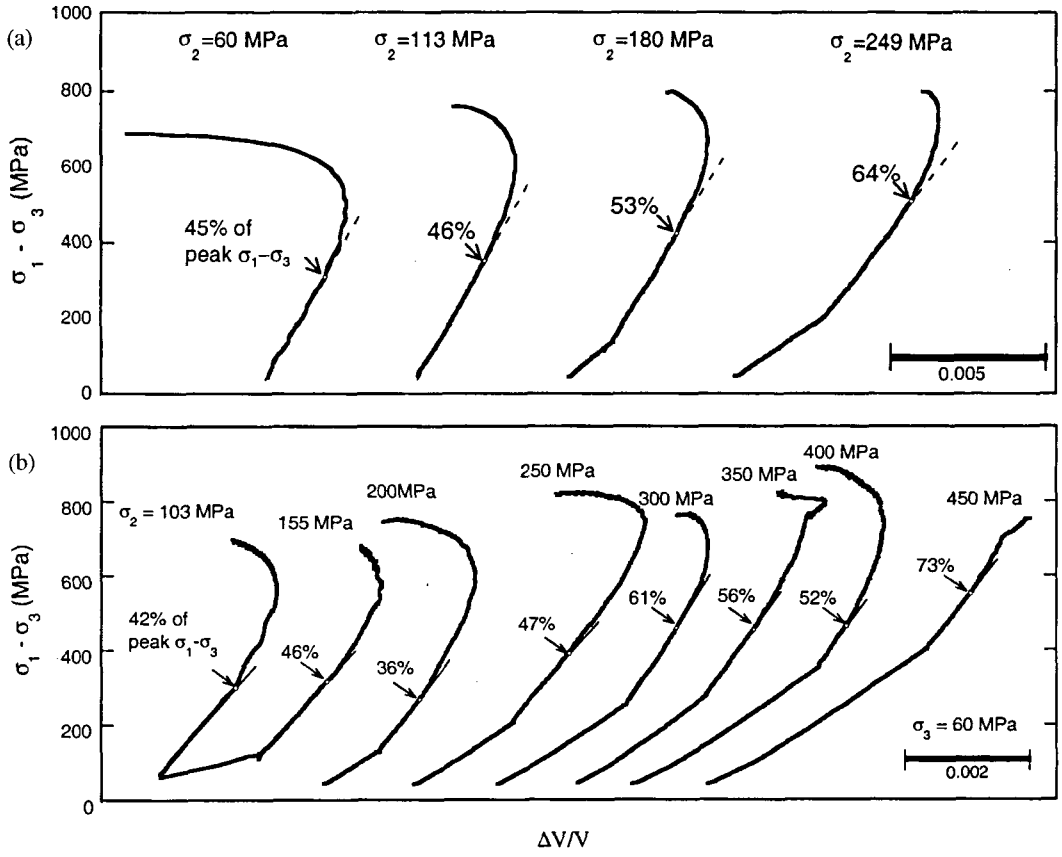


**Fig. 7.** Stress ($\sigma_1 - \sigma_3$) variation with volumetric strain $\Delta V/V$ and dilatancy onset (pointed by arrows) for different (2 magnitudes and constant $\sigma_3$ (60 MPa) in (a) Westerly granite and (b) KTB amphibolite.

eventual failure, are subparallel to the $\sigma_1 - \sigma_2$ plane and open up primarily in the $\sigma_3$ direction.

Another mechanical property common to both rocks is the post peak (also called post failure) stress-strain behavior, which can be characterized as class II, following Wawersik and Brace (1971). In these crystalline rocks the maximum principal stress $\sigma_1$ and the strains in the $\sigma_1$ and $\sigma_2$ directions are reduced after the peak stress is reached, while the strain in the $\sigma_3$ direction keeps growing, indicating increased cracking or widening in the $\sigma_3$ direction of previously developed cracks (Fig. 6).

Fig. 7 depicts the relationship between stress ($\sigma_1 - \sigma_3$) and volumetric strain $\Delta V/V$ (the summation of all three principal strains). The plots show the extent of linear elasticity, characterized by a nearly straight line in the first portion of the loading segment after $\sigma_3$ and $\sigma_2$ have reached their preset values. At some point, the curve becomes nonlinear with the volumetric strain decreasing at a diminishing rate. This phenomenon, known as dilatancy, has been correlated to internal microcracking responsible for expanding the volume and for leading eventually to the creation of the fracture plane (Brace et al., 1966). The point of departure from linearity is defined as the onset of dilatancy. In several tests for which $\sigma_3$ was maintained constant, specifically $\sigma_3 =$ 100 MPa in Westerly granite, and $\sigma_3 = 60$ MPa in KTB amphibolite, the points of dilatancy onset were determined and marked with arrows in Fig. 7. The common phenomenon observed in both rocks is the gradual rise in dilatancy onset with the increase in the magnitude of $\sigma_2$. Since the dilatancy onset is considered an indicator of microcracking emer-

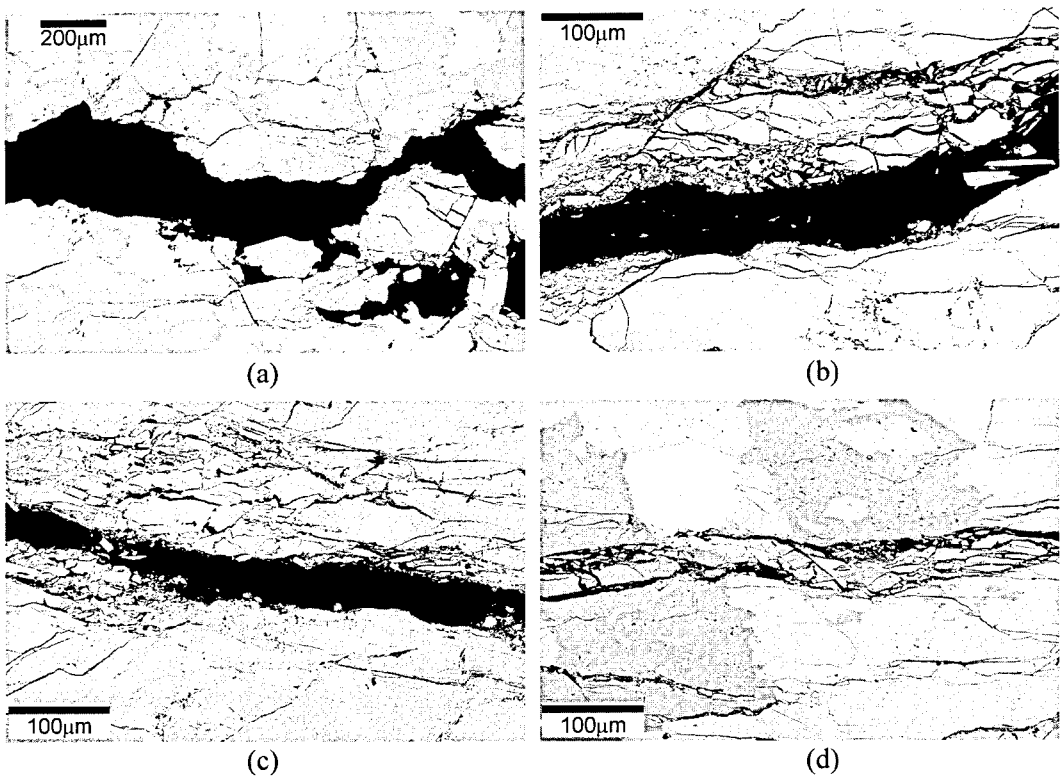


**Fig. 8.** SEM micrographs of cross sections of four specimens tested under the same $\sigma_3$ (=60 MPa) but different $\sigma_2$ magnitudes ($\sigma_2 = 60$, 113, 180, and 249 MPa in (a), (b), (c), and (d), respectively). $\sigma_2$ direction is lateral and $\sigma_3$ direction is vertical. The main fracture in all cases is subparallel to $\sigma_2$. Localized microcracks align themselves gradually with $\sigma_2$ direction as the stress difference ($\sigma_2 - \sigma_3$) increases.

gence, the significance of the trend shown in Fig. 7 is that the increase in the magnitude of the intermediate principal stress extends the elastic range of the stress-strain behavior for a given $\sigma_3$. Since rock compressive failure is considered as the culmination of a progressive development of microcracks, the $\sigma_2$ effect on the onset of dilatancy demonstrates a retardation of the beginning of the failure process, which is perhaps also responsible in part for the higher rock strength.

## Micromechanics of Fracture

In order to see the effect of the intermediate principal stress on micromechanics of brittle fracture, tested samples were inspected using a scanning electron microscope (SEM model JEOL JSM-6100). Sections were cut along planes orthogonal to $\sigma_1$ direction. The sections were ground flat and polished down to 0.05 μm. The surface was then sputter coated with a 0.06-μm-thick carbon layer. Fig. 8 depicts four views of the fracture cross section in Westerly granite tested under the same least horizontal stress $\sigma_3 = 60$ MPa, and $\sigma_2$ varying from 60 to 113 to 180 to 249 MPa. Photomicrographs shown here are oriented with $\sigma_3$ in the vertical, and $\sigma_2$ in the lateral directions. In all cases, the fracture plane is subparallel to $\sigma_2$. All four photomicrographs provide evidence that visible microcracks are localized in the proximity of the main fracture. As the magnitude of $\sigma_2$ is increased from test to test, the localized cracks adjacent to the main fracture seem to align themselves with the direction of the intermediate principal stress. When $\sigma_2 = \sigma_3 = 60$ MPa, the zone immediately near the fault is fragmented into nearly equidimensional blocks created by randomly

oriented cracks, as is expected when these two principal stresses are equal. At $\sigma_2 = 113$ and 180 MPa, many microcracks align themselves to $\sigma_2$ direction. However, numerous microcracks are still randomly oriented, resulting in severe rock fragmentation in the proximity of the main fracture. At $\sigma_2 = 249$ MPa, most microcracks are subparallel to $\sigma_2$ direction. Because of the paucity of microcracks whose strikes are at high angle with respect to $\sigma_2$ direction, there is less tendency of fragmentation. In this photomicrograph, the main fracture is a localized zone in which mutually subparallel microcracks are aligned to $\sigma_2$ direction. This results in a reduced blocky structure, rendering the main fracture considerably narrower for a higher $\sigma_2$. A very similar observation was made in the KTB amphibolite (Chang and Haimson, 2000).

## Conclusions

The two crystalline rocks exhibited substantial similarity in their mechanical behavior. The first important result emerging from the tests is that the effect of the intermediate principal stress $\sigma_2$ on the compressive strength cannot be ignored in crystalline rocks, as is tacitly implied in Mohr-type strength criteria. To the contrary, depending on the level of the least and intermediate principal stresses, rock strength may increase by as much as 50% or more as compared with the strength under the condition used to obtain Mohr-like criteria ($\sigma_2 = \sigma_3$). Generally, the reported tests strongly suggest that use of the conventional Mohr-type criteria in crystalline rocks may lead to overly conservative predictions of strength. Instead, a true triaxial strength criterion that accommodates both tested crystalline rocks can be expressed as the octahedral shear stress at failure as a function of the mean normal stress acting on the developed fault plane. True-triaxial strength experimental points for both the granite and the amphibolite are surprisingly well fitted by a power function in this domain.

Brittle failure under true triaxial stress condition ultimately takes the form of a steeply dipping fault striking in the direction of $\sigma_2$. For the same $\sigma_3$, fault dip angle increases significantly with the magnitude of the intermediate principal stress.

Measurements of strain show accelerated lengthening in the $\sigma_3$ direction with increase in $\sigma_1$. This lengthening is significantly larger than in the $\sigma_2$ direction, suggesting that microcracks subparallel to $\sigma_1$, open mainly in the $\sigma_3$ direction. This inference is supported by SEM micrographs of specimen cross sections in the $\sigma_2 - \sigma_3$ plane. Measured volumetric strain variation with the magnitude of $\sigma_1$ indicates that for the same $\sigma_3$, dilatancy onset generally increases with the rise in the intermediate principal stress, reflecting a widening of the elastic range as the intermediate principal stress is increased for the same least stress. This suggests a retardation of the onset of the failure process, which may in part be responsible for the $\sigma_2$-related increase in strength in both tested crystalline rocks.

## References

Ashby, M.F. and Sammis, C.G., 1990, The damage mechanics of brittle solids in compression. Pure and Applied Geophysics, 133, 489-521.

Brace, W.F., 1964, Brittle fracture of rocks. In Judd, W.R., (ed.), State of Stress in the Earth's Crust, Elsevier, New York, 111-174.

Brace, W.F., Pauling, B.W., and Scholz, C.H., 1966, Dilatancy in the fracture of crystalline rocks. Journal of Geophysical Research, 71, 3939-3953.

Chang, C. and Haimson, B., 2000, True triaxial strength and deformability of the German Continental Deep Drilling Program (KTB) deep hole amphibolite. Journal of Geophysical Research, 105, 18999-19013.

Drucker, D.C. and Prager, W., 1952, Soil mechanics and plastic analysis or limit design. Quarterly of Applied Mathematics, 10, 157-165.

Ewy, R.T., 1998, Wellbore stability predictions using a modified Lade criterion. In Proceedings of Eurock 98: SPE/ISRM Rock Mechanics in Petroleum Engineering, Society of Petroleum Engineers, 1, SPE/ISRM paper no. 47251, 247-254.

Freudenthal, A., 1951, The inelastic behavior and failure of concrete. In Proceedings of First U.S. National Congress of Applied Mechanics, American Society of Mechanical Engineers, New York, 641-646.

Hoek, E. and Brown, E.T., 1980, Empirical strength criterion for rock masses. Journal of Geotechnical Engineering. ASCE, 106, 1013-1035.

Jaeger, J.C. and Cook, N.G.W., 1979, Fundamentals of Rock Mechanics, 3rd ed., Chapman and Hall, New York, 593 p.

Krech, W.W., Henderson, F.A., and Hjelmstad, K.E., 1974, A standard rock suite for rapid excavation research. Bureau of Mines Report of Investigations no. 7865, 29 p.

Lockner, D.A., Byerlee, J.D., Kuksenko, V., Ponomarev, A., and Sidorin, A., 1991, Quasi-static fault growth and shear fracture energy in granite, Nature, 350, 39-42.

McGarr, A. and Gay, N.C., 1978, State of stress in the earth's crust. Annual Review of Earth and Planetary Sciences, 6, 405-436.

Mogi, K., 1971, Fracture and flow of rocks under high triaxial compression, Journal of Geophysical Research, 76, 1255-1269.

Nadai, A., 1950, Theory of Flow and Fracture of Solids, 1, McGraw-Hill, New York.

Quinn, A.W., 1954, Bedrock geology of Rhode Island. Transactions of the New York Academy of Sciences, 264-269.

Rauen, A. and Winter, H., 1995, Petrophysical properties. In KTB Report 95-2, Niedersachsisches Landesamt fur Bodenforschung, Hannover, Germany, D1-D45.

Reches, Z. and Dieterich, J.H., 1983, Faulting of rocks in three-dimensional strain fields 1. failure of rocks in polyaxial, servo-control experiements. Tectonophysics, 95, 111-132.

Rockel, T. and Natau, O., 1995, Rock mechanics. In KTB Report 95-2, Niedersachsisches Landesamt fur Bodenforschung, Hannover, Germany, E1-E9.

Scholz, C.H., 1990, The Mechanics of Earthquakes and Faulting, Cambridge University Press, New York, 439 p.

Takahashi, M. and Koide, H., 1989, Effect of the intermediate principal stress on strength and deformation behavior of sedimentary rocks at the depth shallower than 2000 m. In Maury, V. and Fourmaintraux, D., (eds.), Rock at Great Depth, A.A.Balkema, Netherlands, 19-26.

Vernik, L. and Zoback, M.D., 1992, Estimation of maximum horizontal principal stress magnitude from stress-induced well bore breakouts in the Cajon Pass scientific research borehole. Journal of Geophysical Research, 97, 5109-5119.

Vernik, L., Lockner, D., and Zoback, M.D., 1992, Anisotropic strength of some typical metamorphic rocks from the KTB pilot hole, Germany. Scientific Drilling, 3, 151-160.

Wawersik, W.R. and Brace, W.F., 1971, Post-failure behavior of a granite and diabase. Rock Mechanics, 3, 61-85.

Wiebols, G.A. and Cook, N.G.W., 1968, An energy criterion for the strength of rock in polyaxial compression. International Journal of Rock Mechanics and Mining Science and Geomechanics Abstracts, 5, 529-549.

Wong, T.F., 1982, Micromechanics of faulting in Westerly granite. International Journal of Rock Mechanics and Mining Science and Geomechanics Abstracts, 19, 49-64.

Manuscript received, November 25, 2003
Revised manuscript received, January 15, 2004
Manuscript accepted, January 30, 2004